NASA Technical Paper 3402

December 1993

Surface Compositional Variations of Mo-47Re Alloy as a Function of Temperature

S. J. Hoekje,
R. A. Outlaw,
and S. N. Sankaran

NASA Technical Paper 3402

1993

Surface Compositional Variations of Mo-47Re Alloy as a Function of Temperature

S. J. Hoekje
Analytical Services & Materials
Hampton, Virginia

R. A. Outlaw
Langley Research Center
Hampton, Virginia

S. N. Sankaran
Analytical Services & Materials
Hampton, Virginia

Acknowledgments

The assistance of Dr. Geoffrey Malafsky of the Naval Research Laboratory, Washington, DC, with XPS investigations is appreciated. The difficult photomicroscopy was performed by R. K. Herrmann.

Abstract

Molybdenum-rhenium alloys are candidate materials for the National Aero-Space Plane (NASP) as well as for other applications in generic hypersonics. These materials are expected to be subjected to high-temperature (above 1200°C) casual hydrogen (below 50 torr), which could potentially degrade the material strength. Since the uptake of hydrogen may be controlled by the contaminant surface barriers, a study of Mo-47Re was conducted to examine the variations in surface composition as a function of temperature from 25°C to 1000°C. Pure molybdenum and rhenium were also examined and the results compared with those for the alloy. The analytical techniques employed were Auger electron spectroscopy, electron energy loss spectroscopy, ion scattering spectroscopy, and X-ray photoelectron spectroscopy. The native surface was rich in metallic oxides that disappeared at elevated temperatures. As the temperature increased, the carbon and oxygen disappeared by 800°C and the surface was subsequently populated by the segregation of silicon, presumably from the grain boundaries. The alloy readily chemisorbed oxygen, which disappeared with heating. The disappearance temperature progressively increased for successive dosings. When the alloy was exposed to 800 torr of hydrogen at 900°C for 1 hour, no hydrogen interaction was observed.

Introduction

Polycrystalline Mo-47Re alloy (weight percent) is a candidate material for advanced hypersonic applications, such as the National Aero-Space Plane (NASP), because of its strength and stability in a high-temperature hydrogen environment. This alloy is proposed for use in the vehicle's hydrogen-fueled engine, with temperatures around 1250°C and a duty cycle of 12 hours. It is also being considered for use as a heat exchange element for solar heating of hydrogen. Past research with the titanium-aluminum alloys has revealed the important role surface effects have on hydrogen interaction and transport and suggest a similar study is warranted for molybdenum-rhenium alloys (refs. 1 and 2).

Rhenium is highly soluble in molybdenum and is added to body-centered-cubic (bcc) refractory metals to improve strength and weldability (ref. 3). The brittleness of molybdenum-rhenium alloys, associated with the sigma phase, is avoided by keeping the rhenium content below 50 percent by weight (refs. 4 and 5). The resulting structure exhibits a fine, homogeneous recrystallized microstructure.

In the past, these alloys have received little attention. Work has been done on superconductivity (refs. 6 and 7) and work function investigations (ref. 8). Recently, work has been done on $Mo_{0.75}Re_{0.25}(001)$, examining surface segregation of molybdenum with low-energy alkali ion scattering (ref. 9).

Molybdenum, usually as a single crystal, has been extensively examined with a variety of surface analytical techniques. These include Auger electron spectroscopy (AES) and low-energy electron diffraction (LEED) (refs. 10 and 11), electron energy loss spectroscopy (EELS) (ref. 12), and X-ray photoelectron spectroscopy (XPS) (refs. 13 and 14). These investigations have focused on variations in kinetics and phase formation for differing surface planes of molybdenum-oxygen reactions, conditions for surface reconstruction, adsorption isotherms, sticking coefficients, and thermodynamic data.

Prior work on rhenium is much less plentiful, perhaps because of the cost and scarcity of this element. Almost all work has been with ribbon filaments or foils of polycrystalline rhenium. No AES, EELS, or ion scattering spectroscopy (ISS) spectra of rhenium-oxygen interaction could be found in the literature. There are some studies on oxygen-surface interactions and thermochemical data for rhenium and rhenium oxides.

The purpose of this investigation was to observe the changes in surface composition of Mo-47Re alloy in ultrahigh vacuum (UHV) as a function of temperature and to ultimately correlate its impact on hydrogen transport. The constituent elements

of molybdenum and rhenium were similarly investigated to provide further understanding of the alloy behavior. To investigate the interaction of hydrogen with the alloy, samples were annealed at 900°C in 800 torr of hydrogen. The analytical techniques of AES, EELS, ISS, and XPS were employed to investigate the surface over the temperature range of 25°C to 1000°C. Further, since the alloy and elements readily oxidize, it was also important to characterize the initial oxidation behavior and to examine the effectiveness of platinum coating and cladding as a protective layer.

Symbols and Abbreviations

AES	Auger electron spectroscopy
bcc	body-centered cubic
CMA	cylindrical mirror analyzer
E	measured energy of particle
E_o	energy of incoming ions
EELS	electron energy loss spectroscopy
$I_{n,i}$	Auger current from element i on nth layer
$I(z)$	fraction of total AES signal that is generated between surface and depth z
ISS	ion scattering spectroscopy
LEED	low-energy electron diffraction
$N(E)$	counts as function of energy
NASP	National Aero-Space Plane
s_o	sticking coefficient at time $t = 0$
$s(\theta)$	sticking coefficient as a function of coverage
t	time, sec
UHV	ultrahigh vacuum
X	element or species of sample
XPS	X-ray photoelectron spectroscopy
z	depth, nm
Θ_{BS}	ISS backscattering angle, deg
Θ_{FS}	ISS forward-scattering angle, deg
θ	surface coverage
λ	electron inelastic mean free path, nm
ν	oxygen flux to surface, cm^{-2}-sec^{-1}
σ	sigma phase of molybdenum-rhenium phase diagram
σ_m	density of bonding sites on surface, cm^{-2}
χ	chi phase of molybdenum-rhenium phase diagram

Experimental Procedure

The polycrystalline samples of Mo-47Re, created by combining molybdenum and rhenium powder and forming with the hot isostatic pressure (HIP) process, were obtained from Sandvik Rhenium Alloys, Inc. Atomic-emission spectroscopy analysis using an inductively coupled plasma was performed on the molybdenum and rhenium constituent powders. The analysis revealed a maximum total impurity level below 500 ppm. Polycrystalline sheets of pure molybdenum and rhenium (from Aldrich Chemical Co., Inc., 99.85 percent pure) were also examined. Samples approximately 1 mm thick with a surface area of 0.25 cm^2 were sequentially polished to a 2000 finish and etched for 40 sec in a solution of 4 percent HF and 10 percent HNO_3. Platinum cladding (150 μm thick) was applied by HIP diffusion bonding, and Pt coating (100 nm thick) by vacuum deposition.

The microstructures of the Mo-47Re, molybdenum, and rhenium samples are shown in figure 1. The molybdenum grains vary in size from about 15 to 80 μm, with an average of about 45 μm, and are relatively free of strain defects. The rhenium has a very broad grain size distribution that extends from a few to several hundred micrometers. It is unclear why the distribution is so broad, but the microstructure has the appearance of the beginning of recrystallization with some degree of grain growth. The smaller grains in the rhenium exhibit some twinning that might suggest the rhenium was heavily cold worked. During heat treatments to 1000°C, recrystallization occurred. The Mo-47Re has a similar microstructure to that of pure molybdenum but has more of an equiaxed appearance. The average grain size is about 20 μm, and there are some defects located primarily at the grain boundaries. These defects are only a few micrometers in diameter and may be the result of trapped gas or some other inclusion revealed during polishing. They also may be regions of second-phase precipitates (σ or χ phase) that are rhenium rich in accordance with the molybdenum-rhenium phase diagram. The differential etching response of the precipitates to the Kroll's reagent used for sample preparation of the photomicrographs could cause the observed pits.

The UHV system has AES, EELS, and ISS capabilities with energy analysis performed with a

single-pass cylindrical mirror analyzer (CMA) and an operating pressure of 2×10^{-10} torr. Samples were heated resistively and the temperature could be elevated to greater than 1000°C in front of any diagnostic system in the chamber. Similar heating capability was also available in the preparation-introduction chamber. The details of the system have been reported in reference 15. The AES and EELS were performed with a 1-V peak-to-peak modulation voltage and used a lock-in amplifier in the first-derivative mode. A primary beam of 5 keV and 1 μA was used for AES, and a beam of 200 eV and 1 μA for EELS. The ISS ($\Theta_{FS} = 68°$ and $\Theta_{BS} = 152°$) was performed with $^4He^+$ ions and $^{40}Ar^+$ ions with a beam energy of 1600 eV and a sample flux of 0.1 $\mu A/cm^2$. The data were acquired in an analog mode for AES and EELS and in a pulse-counting mode for ISS. The analog signals were converted to digital data and processed with digital filtering techniques (ref. 16). The AES data were normalized to the dominant metal peak, usually molybdenum 186 eV ($M_5N_{2,3}N_{4,5}$) or rhenium 161 eV ($N_5N_4N_4$). The XPS data were acquired in a comparable system with a double-pass CMA operating in the retarding mode with an Al (Kα) anode X-ray source.

The samples were heated to 1000°C, in 100°C steps, and held at a given temperature for 20 minutes before data were acquired. This time was found to be sufficient for signal levels to stabilize. Oxygen dosing was done at 50°C in the main chamber by backfilling with oxygen to a partial pressure of approximately 3×10^{-9} torr. Hydrogen dosing was done in the sample-prep chamber at a pressure of 800 torr and a temperature of 900°C for 1 hour. The oxygen dosing conditions were chosen such that saturation occurred in about 10 minutes. To maximize the probability of interaction, the hydrogen dosing was done at the maximum temperatures and pressures the sample-prep chamber could tolerate. Sputtering, with $^{40}Ar^+$ ions, was done with a beam energy of 3 keV and a flux of about 10 $\mu A/cm^2$.

The hydrogen uptake behavior of the Mo-47Re alloy was studied with the UHV microbalance technique described in reference 17. The specimen, in the form of a coupon with the dimensions 10 mm by 1 mm by 1 mm, was hung from a microbalance inside a UHV chamber and heated to 1100°C prior to hydrogen exposure to expel any residual hydrogen. After this treatment the specimen was maintained at 900°C and exposed to hydrogen at 250 torr while the weight gain of the sample was continuously monitored through the microbalance. The microbalance had a sensitivity of 1 μg and could determine weight changes of 10 μg accurately. Tests were run until no more weight changes could be detected by the microbalance.

Results and Discussion

As-Received Surface Composition

The AES, ISS, and XPS spectra of as-received Mo-47Re alloy are presented in figures 2 to 4. The surface consists of a mixture of native oxides and adventitious carbon, which were probably formed during the HIP processing. The molybdenum features dominate the AES spectra and rhenium cannot be observed. This dominance of the molybdenum features probably occurs because the bulk concentration of molybdenum is approximately twice that of rhenium and the molybdenum AES sensitivity factor is six times that of rhenium (ref. 18). The AES data reveal a surface concentration that is approximately 50 percent (atomic) oxygen, 25 percent (atomic) carbon, and 25 percent (atomic) molybdenum.

The ISS ($^4He^+$) spectra in figure 3 reveal a surface consisting of predominantly oxygen, fluorine, molybdenum, and rhenium. Since ISS is extremely surface sensitive, sampling the outermost one to two atomic layers, these data represent the true surface constituency more accurately than do the AES data. The sensitivity factors in ISS are difficult to determine but are strongly dependent on the mass of the target atom. The forward-scattering spectrum, which has higher sensitivities but less resolution (ref. 19), shows a surface that is approximately 67 percent (atomic) oxygen; the remaining 33 percent (atomic) is a mixture of molybdenum and rhenium in indeterminable concentrations. The cross section for carbon is too small for a signal to be detected. The backscattering spectrum reveals there is approximately twice as much molybdenum as rhenium, a finding that is consistent with the bulk concentration. The fluorine feature is probably from the etchant employed during sample preparation. If the fluorine is not considered, the data suggest a surface that is 67 percent (atomic) oxygen, 22 percent (atomic) molybdenum, and 11 percent (atomic) rhenium.

The high-resolution XPS spectra, presented in figure 4, reveal the five metallic oxides on the surface. The molybdenum is present as a mixture of 50 percent MoO_2 and 50 percent MoO_3. The rhenium is also present as a mixture of about 50 percent ReO_2 and 50 percent ReO_3, though a small amount of Re_2O_7 is detected. Neither element is present as a free metal.

The AES and ISS spectra of as-received molybdenum do not vary significantly from those of the Mo-47Re alloy except for trace surface contamination by potassium observed with the ISS. The AES spectrum of rhenium in figure 5(a) is distinctly different. No rhenium or oxygen are detectable and the entire surface is covered with carbon. The small, and therefore nondetectable, ion scattering cross section for carbon is apparent from the ISS spectra in figure 5(b). With heating the surface composition changes, and rhenium is detected at 300°C with ISS and at 500°C with AES. However, when allowed to cool to room temperature, the carbon returned and rhenium could not be detected with AES after 30 minutes at room temperature. This rapidly occurring carbon overlayer must have originated within the bulk or the grain boundaries or both. The pressure within the UHV chamber (about 10^{-10} torr) is such that the flux of gas to the surface is not sufficient to saturate it with carbon in so short a period. Rhenium does not form a carbide (ref. 3) and carbon only forms a very dilute solid solution with rhenium (ref. 20), facts that suggest the majority of the carbon is in the grain boundaries.

The Auger current $I_{n,i}$ from element i, originating from the nth layer undergoing an Auger transition, is a complex function of numerous factors including the geometry, the beam irradiating process, the atom density and element concentration, the escape depth of the AES electron, the ionization cross section of the atom, and the Auger transition probability (ref. 21). A simplified model of the process, considering only the escape depth of the AES electron, can be written as

$$I(z) = 1 - \exp(-z/\lambda) \qquad (1)$$

where

$I(z)$	fraction of AES signal originating in region between surface and depth z
λ	inelastic mean free path, nm
z	depth, nm

The rhenium 161-eV peak has an inelastic mean free path of approximately 0.6 nm (ref. 22), and table 1, derived from equation (1), suggests that more than 2 nm of carbon are necessary to completely mask the rhenium signal.

Compositional Variations (AES) of As-Received Samples With Temperature

The variations in surface composition as a function of temperature for Mo-47Re, molybdenum, and rhenium are presented in figure 6. The compositions were measured by AES, using peak-to-peak heights and sensitivity factors. These intensities were then normalized with the concentration of the dominant molybdenum or rhenium peak to compensate for instrument fluctuations and overlayer effects. The surface composition of Mo-47Re varies with heating and shows a complete loss of carbon and oxygen and the appearance of silicon at higher temperatures. The pure molybdenum surface changes in a manner similar to that of the alloy, though the oxygen loss is less precipitous and the silicon appears at a higher temperature. Rhenium is distinct from the other two, with a sharp increase and subsequent decrease of silicon, no detectable oxygen, and carbon never completely disappearing.

The complete loss of oxygen by 800°C for the surfaces containing molybdenum is difficult to explain in terms of the metallic oxides. One oxide of rhenium, Re_2O_7, sublimes below 300°C and another, ReO_3, decomposes to ReO_2 and Re_2O_7 when heated in vacuum (ref. 23). Rhenium dioxide, ReO_2, is believed to be stable in vacuum up to 750°C. Molybdenum trioxide, MoO_3, either sublimes at 500°C (ref. 24) or vaporizes around 600°C (ref. 25), though it reduces to the dioxide when heated in hydrogen (ref. 26) and perhaps when heated in vacuum. The compound MoO_2 is very stable in vacuum, surviving up to 1300°C (ref. 27) and perhaps to 1900°C (ref. 25). This behavior suggests that any oxygen on the surface as MoO_2, which XPS reveals is 50 percent of the native molybdenum oxides, should be present throughout the investigation. The loss may be due to the breakup of the native oxide and subsequent dissolution into the bulk.

Carbon completely disappears by 400°C for both molybdenum-containing surfaces. The loss is probably due to desorption as CO or CO_2, dissolution, or both. The reappearance of carbon in Mo-47Re at higher temperatures may be due to an entrainment from the segregating silicon sweeping the carbon out of the grain boundaries to the surface. This entrainment was investigated by sputter annealing at 600°C until the near-surface regions appeared free of carbon. With subsequent heating silicon reaches a maximum at 680°C, 200°C cooler than the initial results presented in figure 6. The carbon was blocking the silicon either in the grain boundaries, at surface sites, or both. The fact that the carbon on the high-temperature (800°C and above) oxygen-free surface does not vanish suggests that at these temperatures disappearance occurs as a volatile carbon oxide.

The room-temperature rhenium surface is covered with carbon, as indicated by AES analysis

in figure 5(a). The AES did not detect rhenium until 500°C and silicon until 600°C. Unlike the molybdenum-bearing samples, however, the silicon concentration substantially decreases at high temperatures, probably because of dissolution since the vapor pressure of silicon is small and the oxide and carbide, if present, are extremely stable. Carbon never totally leaves the surface, either because of strong chemisorption, insolubility, the necessity of oxygen to form a volatile, or a combination of the preceding effects. In earlier work with single-crystal Re(0001), the surface was cleaned of all contaminants by vacuum annealing at 1500°C (ref. 28).

One unusual observation in this work is the trace amount of sulfur; in the titanium alloys, sulfur is the most noticeable segregant (ref. 29). In previous work on single-crystal molybdenum, large sulfur concentrations have been observed (ref. 30). The molybdenum-rhenium surface had trace quantities of sulfur at 400°C which disappeared by 600°C.

Oxygen Adsorption to Saturation

The AES spectra of the three annealed, sputter-cleaned materials are shown in figure 7. The only rhenium feature observable in Mo-47Re is the peak at 176 eV ($N_5O_3O_3$), located between two dominant molybdenum peaks at 161 eV ($M_4N_1N_{4,5}$) and 186 eV ($M_5N_{2,3}N_{4,5}$). The AES spectra of Mo-47Re did indicate rhenium at the higher energies of 1799 eV ($M_5N_7N_7$), but the low-energy feature at 33 eV ($N_7O_{4,5}O_{4,5}$) was masked by the molybdenum peak at 28 eV ($N_{2,3}VV$); neither of these features are shown as they add no new information. During all subsequent investigations no AES feature displayed any shape change except the molybdenum valence transition below 100 eV and a molybdenum core transition at 122 eV ($M_5N_1N_3$) (ref. 31). The AES features of at least four molybdenum peaks (28 eV, 161 eV, 186 eV, and 221 eV) undergo peak shape changes with oxidation (refs. 31 and 32), but only the molybdenum peak at 28 eV changes in this investigation.

All three surfaces were dosed to saturation with oxygen at approximately 50°C and a partial pressure of 3×10^{-9} torr. These experiments were repeated several times to ensure accuracy. While the as-received Mo-47Re surface contained copious amounts of oxides of molybdenum and rhenium (as revealed in the XPS spectra of fig. 4), all attempts to grow oxides in the UHV chamber were unsuccessful in this investigation. High-resolution XPS examination of the alloy after oxygen dosing (up to 1000 Langmuirs), from room temperature to 800°C, failed to detect any metallic oxides. The literature suggests that growth of molybdenum oxides at UHV pressures occurs between 750°C and 1200°C on single-crystal surfaces (refs. 11, 27, and 31), though one report indicates growth at 550°C (ref. 33). The AES spectra of all three dosed surfaces are presented in figure 8. The molybdenum and Mo-47Re surfaces have approximately four times more chemisorbed oxygen than the rhenium surface has. The adsorption curves for the three surfaces are presented in figure 9. Oxygen adsorbs more readily on Mo-47Re than on the constituent elements. The adsorption curve of rhenium most closely resembles the behavior of the alloy, an observation that suggests rhenium may be the rate-limiting adsorption site in the oxygen chemisorption on Mo-47Re. Although only chemisorption is occurring here, the Gibb's free energy of oxide formation in table 2 suggests a greater probability of the oxygen being with the rhenium than with the molybdenum (ref. 34).

Adsorption studies of oxygen on molybdenum revealed a marked influence of crystal orientation on adsorption rate (refs. 10 and 11). The high-temperature study (at about 750°C) of Zhang et al. showed that the Mo(111) surface adsorbs a monolayer six times faster than the Mo(100) plane does. Bauer and Poppa's study (ref. 10), performed at room temperature, revealed that polycrystalline molybdenum adsorbed oxygen more slowly than the (111), (001), or (110) planes do. The slow adsorption rate of the polycrystalline surface indicates a dissociative limitation because of misorientation of the grains at the surface, which has mostly high-index planes. Both studies, as well as others (refs. 13 and 30), have observed the linear region at low coverage of the molybdenum-oxygen adsorption curve, consistent with figure 9.

Sticking coefficients for the three surfaces are presented in figure 10. The curves were calculated by assuming the adsorption curves in figure 9 were equivalent to coverage θ as a function of time (for a given pressure) and determining $d\theta/dt$ as a function of time. Thus,

$$\frac{d\theta}{dt} = s_o\,(1-\theta)\,\nu/\sigma_m = s\,(\theta)\,\nu/\sigma_m \qquad (2)$$

where

θ	surface coverage
t	time, sec
s_o	sticking coefficient at $t = 0$
$s(\theta)$	sticking coefficient as function of coverage
ν	oxygen flux to surface, cm^{-2}-sec^{-1}
σ_m	density of bonding sites on surface, cm^{-2}

The Mo-47Re and rhenium curves are very similar and describe a surface that is highly reactive with oxygen. The dependence of the sticking coefficient on coverage at low coverage values is atypical but has been previously observed with oxygen on rhenium (ref. 35). An early study of gas-solid interactions with noble gas molecular beams has compared the molybdenum-oxygen and the rhenium-oxygen chemistry (ref. 36). The study concluded that the molybdenum-oxygen behavior was analogous to tungsten-oxygen and involved at least two distinct bonding site energies. Though no specific model was offered for the rhenium-oxygen behavior, it was observed to be significantly different from molybdenum-oxygen interaction and may involve only one bonding site energy. The present work supports the conclusion that oxygen interaction with molybdenum differs significantly from that with rhenium.

Oxygen Disappearance With Increasing Temperature

Oxygen-saturated surfaces were subsequently heated from room temperature to 1000°C while surface composition was monitored. The behavior of the molybdenum and rhenium samples was repeatable for all three runs and is presented in figure 11. The rhenium surface is free of oxygen by 600°C, and the molybdenum surface by 800°C. This is the same trend as that observed for the oxides, where the rhenium oxides sublime or decompose at least 200°C lower than do the molybdenum oxides.

The influence of temperature on surface oxygen concentration for Mo-47Re is presented in figure 12. The alloy behavior is distinct from that of either element. The disappearance temperature for the alloy increases with successive cycles; the native oxide is gone by 800°C, while the dosed surface oxygen progressively disappears at ever higher temperatures (1000°C for the third cycle). This temperature effect suggests that some, if not all, of the oxygen leaves the surface of the alloy by dissolution, the process requiring greater temperatures for removal as the near-surface region becomes more and more oxygen saturated. This effect has also been observed for oxygen behavior with Ni(110) (ref. 37). The nickel is well known to dissolve oxygen, and this dissolution required higher and higher temperatures with each dosing cycle.

Another observation for this system is the enrichment of molybdenum at the surface of Mo-47Re with high temperatures. From ISS, the ratio of molybdenum to rhenium increased above 500°C, and by 800°C the surface was 30 percent richer in molybdenum. By 1000°C, the molybdenum enrichment decreased to 15 percent of the original room temperature ratio. The heat of solution of molybdenum in rhenium is −20 kJ/mol (ref. 38), which is consistent with the apparent mobility observed in this and previous investigations (i.e., refs. 8 and 9). The mobile molybdenum may enhance the dissolution of the chemisorbed oxygen observed in figure 12.

Auger Peak Shape Change of Molybdenum With Temperature and Oxygen Exposure

As previously mentioned, XPS did not reveal any shifts in binding energy of chemisorbed Mo-47Re as compared with that of the sputter-cleaned Mo-47Re, but the low-energy molybdenum AES peaks, which involve valence electrons, are sensitive to the molybdenum chemical state (ref. 32). Six features are noticeable in low-energy AES spectra of a sputter-cleaned surface (fig. 13): three unidentified features at 8 eV, 14 eV, and 34 eV and three known AES transitions at 20 eV ($NN_{2,3}V$), 32 eV ($N_{2,3}VV$), and 45 eV (N_1VV). Oxygen chemisorption results in a reduction in the intensity in the three unidentified peaks. Annealing Mo-47Re to 1000°C and then cooling the sample to room temperature generates a spectrum that is the same as that of the oxygen-dosed surface in figure 13. It appears that the damage done to the surface by sputtering has been reconstructed by the low-temperature chemisorption, a finding that has been previously reported for Mo(100) (ref. 13).

A more detailed examination of the chemisorbed surface with temperature (fig. 14) reveals significant chemical changes. The unidentified peak at 14 eV is noticeable at 400°C, reaches maximum intensity at 500°C, and is still detectable at 800°C. The temperature of maximum intensity (500°C) is the point where the ISS detected the start of surface enrichment in molybdenum. Whether these two are related is not apparent. Figure 14 also reveals a gradual disappearance of the unidentified feature at 8 eV and the decrease in the transition at 45 eV with heating. The low-energy features return to their initial conditions when the surface is allowed to cool.

A very distinct and permanent peak shape change occurs for the molybdenum transition at 122 eV ($M_5N_1N_3$) with heating (fig. 15). The peak is normally split into two peaks with negative incursion of comparable intensity (doublet: $^3D_{5/2}-^4S_{1/2}-^4P_{1/2}$ and $^3D_{3/2}-^4S_{1/2}-^4P_{1/2}$) (ref. 31). This feature is invariant with exposure to oxygen or the presence of known contaminants (carbon, potassium, or silicon), probably because it is a core level transition.

However, when the material is heated to 1000°C for 20 minutes, the shape of the peak dramatically changes, with a decrease in the transition associated with the $^3D_{3/2}$ state and a corresponding increase in the transition associated with the $^3D_{5/2}$ state. The change in peak shape, perhaps due to a phase alteration or a surface relaxation from annealing, remained when the sample was cooled to room temperature, and days later the peak had not returned to its original shape. With mild sputtering, the transition reverted to the initial shape. The change was observed in both the molybdenum and the Mo-47Re alloy.

Silicon Segregation With Temperature and Its Influence on Oxygen Adsorption

Silicon is a common impurity of molybdenum, rhenium, and Mo-47Re. As shown in figure 16, the silicon segregation curve as a function of temperature for Mo-47Re is nearly identical to the sum of the silicon concentration curves of molybdenum and rhenium. The rhenium sample used in this investigation had a maximum silicon to rhenium atomic ratio of 0.3, whereas the molybdenum sample had four times more silicon with a ratio of 1.2. Given that the alloy has approximately twice as many molybdenum atoms as rhenium atoms and the trend observed with the pure elements, it is reasonable to assume that most of the silicon in the alloy came from the molybdenum. Based on Holloway's arguments concerning the electron inelastic mean free path (ref. 39), the maximum silicon segregation coverage on the Mo-47Re was 1.7 monolayer. The silicon is believed to segregate to the grain boundaries and diffuse to the surface at higher temperatures. This view is supported by the previous observations on surface compositional changes with temperature (fig. 6). The silicon segregation may be impeded by the carbon in the grain boundary because when the silicon appears, carbon also appears, apparently entrained by the mobile silicon. The emergence of the silicon is clearly mirrored by the loss of oxygen on the surface, an indication that segregation did not occur until surface sites became available. Similar behavior has been observed in the titanium aluminides, for which sulfur segregation only occurs when the carbon and oxygen have substantially disappeared from the surface (ref. 29).

Since silicon is present and stable at high temperatures in the molybdenum-bearing samples, the possibility of forming silica *in situ* as a barrier film for protecting Mo-47Re from oxidation was examined. Figure 17 reveals that at room temperature, silicon on Mo-47Re reduces the oxygen saturation level by 75 percent. The oxygen saturation level of pure molybdenum at room temperature (not shown) is decreased by 90 percent when silicon is present. The silicon disappears from the pure rhenium surface at high temperatures (apparently by dissolution), so a silicon saturated surface was not available for examining. The mechanism for inhibiting oxygen adsorption on the molybdenum-bearing samples is not clear. The ability of the oxygen-dosed, silicon-segregated surfaces to avoid oxidation was examined by heating (to 600°C) in the UHV chamber for 5 minutes with an oxygen partial pressure of 1×10^{-8} torr. The resulting samples were not protected by the coating. No silicon was detected on the surface after high-temperature oxygen exposure. However, AES analysis of silicon may not be a reliable indicator of concentration. The silicon transition at 92 eV (L_3VV) involves valence electrons and the decrease in the signal with oxygen exposure may be an artifact due to the decreased probability of the valence electrons involved in chemical bond formation participating in the AES process.

A more detailed examination of the interaction of oxygen with the silicon-saturated Mo-47Re with EELS and ISS (using $^4He^+$ ions in the backscattered mode) is presented in figures 18 and 19. The main features in EELS are surface and bulk plasmons, core level electron transitions, and valence level electron transitions. The most distinctive change with temperature in figure 18 is at 3 eV. The other features are relatively stable. It is difficult to assign these features, though the one at 35 eV corresponds with a molybdenum core level transition (ref. 40).

From the ISS results (fig. 19), the disappearance of the EELS 3-eV feature coincides with the loss of oxygen and the appearance of silicon and rhenium on the surface, a combination that suggests the low-energy EELS feature is due to an oxygen-surface bond. The ISS spectra at low temperatures are essentially oxygen and molybdenum. The high temperature is free of oxygen, with the disappearance mirroring the appearance of silicon and rhenium. Oxygen has preferentially chemisorbed on silicon and rhenium. Assuming comparable cross sections, the ISS peak height ratio of molybdenum to rhenium would be the same as the atomic ratio, about 2. Analysis of a sputter-cleaned, annealed surface (not shown) reveals a molybdenum to rhenium peak height ratio of about 2.5. When silicon is present the ratio increases to about 4 (upper spectrum, fig. 19), an implication that the silicon has preferentially covered the rhenium.

Platinum Cladding for Oxygen Protection

A platinum cladding (150 μm) was applied to the Mo-47Re as a barrier against high-temperature oxygen degradation. The clad sample was then heated to 1250°C for 12 hours in an arc-jet-heated air environment. The sample was analyzed by AES and ISS and no molybdenum or rhenium was detected, either on the surface or after 1 hour of sputtering. Previous experience suggested the 1-hour sputtering removed about 3 μm of material. The sample was then heated, in vacuum, to 800°C for 3 hours and examined with AES. The Auger spectrum of the platinum-cladded sample after heating is presented in figure 20. Two molybdenum features are observable, one at 122 eV and one at 148 eV. Apparently no molybdenum was detected in the first experiment because the oxides had undergone volatile desorption in the arc jet. The fact that no molybdenum was observed after sputtering strongly indicates that the molybdenum diffusion was in the grain boundaries or in the defects of the coating, which had a small area fraction that was not detectable by AES or ISS. The second experiment with heating in UHV allowed the molybdenum to accumulate on the surface to a detectable level.

To further examine the interaction of platinum with Mo-47Re, a separate piece of Mo-47Re was vacuum deposited with 100 nm of platinum. No molybdenum or rhenium was detected on the surface after coating. The sample was heated to 600°C in vacuum, and after 10 minutes a large molybdenum peak was detected. Increasing the temperature to 800°C generated a molybdenum surface concentration that was so large no AES platinum peaks were detected between 100 and 250 eV. Assuming the cross sections are equivalent, the ISS revealed a surface of approximately 80 percent molybdenum and 20 percent platinum. No rhenium was detected by AES or ISS, so molybdenum probably diffused through the platinum instead of the platinum dissolving in the bulk.

Interaction of Hydrogen With Mo-47Re

A sputter-cleaned Mo-47Re sample was exposed to 800 torr of hydrogen for 1 hour at 900°C. The surface was then examined using AES, EELS, and ISS. No changes were detected.

To investigate whether hydrogen uptake occurs with this alloy, a sample was exposed to 25 torr of hydrogen for 96 hours at 900°C. Within the limitations of the instrumentation (i.e., minimum detectable weight change of 10 μg), no discernible weight gain was observed. Because of the limitations of the furnace and the large volume of the system, tests at higher temperatures and higher pressures could not be conducted.

Theoretical calculations with a multiple-scattering, local-density, functional-cluster technique showed that the Mo-47Re structure repels the hydrogen atom (ref. 41). The formation of atomic hydrogen is required for dissociative adsorption, the dominant mechanism for molecular hydrogen chemisorption. Since adsorption is the first step in hydrogen transport (ref. 1), these results are consistent with the lack of hydrogen transport observed in the present investigation.

Summary of Results

The examined Mo-47Re alloy had bulk contaminants of carbon, oxygen, silicon, and traces of sulfur. The native surface was carbon and oxygen rich with traces of fluorine and potassium. The grain boundary segregant silicon was not substantially removed with heating, though there was a decrease at 1000°C. Silicon is a common contaminant of both molybdenum and rhenium, and its variation with temperature in Mo-47Re was consistent with its behavior in the constituent elements. All other contaminants disappeared when the samples were heated to 800°C.

Oxygen adsorbed more quickly on Mo-47Re than on either molybdenum or rhenium. The oxygen disappearance with temperature from molybdenum and rhenium was repeatable and suggests loss through the gas phase, while the Mo-47Re sample required an increase in temperature for oxygen disappearance for each successive exposure, a result that suggests that at least some of the oxygen was dissolving.

The Gibb's free energy of formation of rhenium oxide, the similarity of the rhenium adsorption curve to the Mo-47Re adsorption curve, and the ion scattering spectroscopy (ISS) spectra revealing oxygen covering all the rhenium sites suggest that rhenium was involved in the rate-limiting step for oxygen incorporation. Molybdenum enrichment occurred at higher temperatures, and the apparent dissolution of oxygen in Mo-47Re may have been enhanced by the mobile molybdenum. Silicon contaminated surfaces of molybdenum and Mo-47Re adsorbed less oxygen than did the noncontaminated surfaces. This behavior is similar to the influence sulfur has on oxygen adsorption on pure molybdenum. Attempts at oxidizing the silicon on the surface failed, an indication of very strong chemisorption.

Platinum claddings were partially effective oxygen barriers, decreasing but not stopping the formation of volatile oxides. Molybdenum diffused through

platinum coatings, but no sign of rhenium diffusion or platinum dissolving in Mo-47Re was observed.

No sign of hydrogen adsorption or surface modification was detected.

NASA Langley Research Center
Hampton, VA 23681-0001
November 18, 1993

References

1. Sankaran, Sankara N.; Outlaw, Ronald A.; and Clark, Ronald K.: *Surface Effects on Hydrogen Permeation Through* Ti-*14*Al-*21*Nb *Alloy*. NASA TP-3109, 1991.

2. Sankaran, S. N.; Herrmann, R. K.; Outlaw, R. A.; and Clark, R. K.: Barrier Layer Formation and Its Control During Hydrogen Permeation Through Ti-24Al-11Nb Alloy. *Metall. Trans. A*, vol. 25, no. 1, Jan. 1994, pp. 89–97.

3. Bryskin, Boris D.: Refractory Metals Forum: Rhenium and Its Alloys. *Adv. Mater. & Process.*, Sept. 1992, pp. 22–27.

4. Maykuth, D. J.; Holden, F. C.; and Jaffee, R. I.: The Workability and Mechanical Properties of Tungsten- and Molybdenum-Base Alloys Containing Rhenium. *Rhenium*, B. W. Gonser, ed., American Elsevier Publ. Co., 1962, pp. 114–125.

5. Falbriard, P.; Rochette, P.; and Nicolas, G.: Refractory Materials Likely To Be Used in the Net Divertor Armour. *12th International Plansee Seminar '89*, Volume 1, Metallwerk Plansee GmbH (Reutte, Tirol, Austria), 1989, pp. 657–672.

6. Morin, F. J.; and Maita, J. P.: Specific Heats of Transition Metal Superconductors. *Phys. Rev.*, vol. 129, no. 3, Feb. 1963, pp. 1115–1120.

7. Andreone, A.; Barone, A.; Di Chiara, A.; Mascolo, G.; Palmieri, V.; Peluso, G.; and Di Uccio, U. Scotti: Mo-Re Superconducting Thin Films by Single Target Magnetron Sputtering. *IEEE Trans. Magn.*, vol. 25, no. 2, Mar. 1989, pp. 1972–1975.

8. Gordon, R. L.: The Work Function of Sputter-Formed Re-1%Mo. *J. Appl. Phys.*, vol. 56, no. 3, Aug. 1984, pp. 810–813.

9. Overbury, S. H.; Van den Oetelaar, R. J. A.; and Zehner, D. M.: Surface Segregation in $Mo_{0.75}Re_{0.25}$(001) Studied by Low-Energy Alkali-Ion Scattering. *Phys. Rev. B*, vol. 48, no. 3, July 15, 1993, pp. 1718–1725.

10. Bauer, E.; and Poppa, H.: On the Adsorption of Oxygen on the Mo{110} Surface and Its Vicinals. *Surf. Sci.*, vol. 127, 1983, pp. 243–254.

11. Zhang, C.; Gellman, A. J.; Wang, G. J.; and Somorjai, G. A.: The Influence of Steps on the Oxidation of Molybdenum Single Crystal Surfaces. *Surf. Sci.*, vol. 164, 1985, pp. L835–L838.

12. Stefanov, P. K.; and Marinova, Ts. S.: HREELS Study of the Interaction of Oxygen With a Mo(111) Surface. *Surf. Sci.*, vol. 200, 1988, pp. 26–34.

13. Marinova, Ts. S.; and Stefanov, P. K.: Interaction of Oxygen With a Mo(111) Surface. *Surf. Sci.*, vol. 164, 1985, pp. 196–208.

14. Conner, G. R.: Combination Analysis of Metal Oxides Using ESCA, AES, and SIMS. *J. Vac. Sci. & Technol.*, vol. 15, no. 2, Mar./Apr. 1978, pp. 343–347.

15. Outlaw, R. A.; Peregoy, W. K.; and Hoflund, Gar B.: *Permeation of Oxygen Through High Purity, Large Grain Silver*. NASA TP-2755, 1987.

16. Savitzky, Abraham; and Golay, Marcel J. E.: Smoothing and Differentiation of Data by Simplified Least Squares Procedures. *Anal. Chem.*, vol. 36, no. 8, July 1964, pp. 1627–1639.

17. Sankaran, Sankara N.; Hermann, Rebecca K.; Clark, Ronald K.; and Outlaw, R. A.: Kinetics of Hydrogen Transport Through Ti-15Mo-2.7Nb-3Al-0.2Si(Beta-21S) Alloy. *Beta Titanium Alloys in the 1990's*, Daniel Eylon, Rodney R. Boyer, and Donald A. Koss, eds., The Miner., Met. & Mater. Soc., 1993, pp. 137–145.

18. Davis, Lawrence E.; MacDonald, Noel C.; Palmberg, Paul W.; Riach, Gerald E.; and Weber, Roland E.: *Handbook of Auger Electron Spectroscopy*, Second ed. Perkin-Elmer Corp., 1979.

19. Brongersma, H. H.; Hazewindus, N.; Van Nieuwland, J. M.; Otten, A. M. M.; and Smets, A. J.: Angular-Dependent Ne^+-Ion Scattering From a Solid Au Target. *J. Vac. Sci. & Technol.*, vol. 13, no. 3, May/June 1976, pp. 670–675.

20. Arnoult, William J.; and McLellan, Rex B.: The Solubility of Carbon in Rhodium Ruthenium, Iridium and Rhenium. *Scr. Metall.*, vol. 6, no. 10, Oct. 1972, pp. 1013–1018.

21. Kane, Philip F.; and Larrabee, Graydon B., eds.: *Characterization of Solid Surfaces*. Plenum Press, 1974.

22. Czanderna, Alvin Warren: *Methods of Surface Analysis*. Elsevier Sci. Publ. Co., 1975.

23. Savitskii, E. M.; Tylkina, M. A.; and Povarova, K. B. (Ch. Nisenbaum, transl., and D. Slutzkin, ed.): *Rhenium Alloys*. U.S. Dep. of Commerce, 1970.

24. Floquet, N.; and Bertrand, O.: Superficial Oxidation of Molybdenum at High Pressure and Low Temperature: RHEED and AES Analyses of the Molybdenum Oxide Formation. *Surf. Sci.*, vol. 251/252, 1991, pp. 1044–1051.

25. Samsonov, G. V., ed. (Robert K. Johnston, transl.): *The Oxide Handbook*, Second ed., Plenum Press, 1982.

26. Dufour, L. C.; Bertrand, O.; and Floquet, N.: Chemical Reactivity of (010)MoO_3: A Structural Study of the MoO_2 Formation in Molecular Hydrogen. *Surf. Sci.*, vol. 147, 1984, pp. 396–412.

27. Nozoye, Hisakazu; Matsumoto, Yoshio; Onishi, Takaharu; and Tamaru, Kenzi: Initial Oxidation of Molybdenum

Studied by a High Resolution Auger-Photoelectron Spectrometer. *J. Chem. Soc., Faraday Trans. 1*, vol. 1, 1976, pp. 389–396.

28. Dooley, George J., III; and Haas, T. W.: Some Properties of the Rhenium (0001) Surface. *Surf. Sci.*, vol. 19, 1970, pp. 1–8.

29. Outlaw, R. A.; Lee, W. S.; Sankaran, S. N.; Wu, D.; and Clark, R. K.: Titanium Aluminides—Surface Composition Effects as a Function of Temperature. *Scr. Metall.*, vol. 25, Jan. 1991, pp. 171–176.

30. Lambert, R. M.; Linnett, J. W.; and Schwarz, J. A.: Adsorption of Oxygen on Molybdenum (111): Effect of Trace Impurities. *Surf. Sci.*, vol. 26, 1971, pp. 572–586.

31. Dadayan, K. A.; Kriger, Yu. G.; Tapilin, V. M.; and Savchenko, V. I.: Chemical Shift in the Auger Spectra of Tungsten and Molybdenum During Oxygen Adsorption. *Izv. Akad. Nauk SSSR*, vol. 38, no. 2, 1974, pp. 273–277.

32. Lin, T. T.; and Lichtman, David: AES Studies of Chemical Shift and Beam Effect on Molybdenum Oxides. *J. Vac. Sci. & Technol.*, vol. 15, no. 5, Sept./Oct. 1978, pp. 1689–1694.

33. Zhang, C.; Van Hove, M. A.; and Somorjai, G. A.: The Interaction of Oxygen With the Mo(100) and Mo(111) Single-Crystal Surfaces: Chemisorption and Oxidation at High Temperatures. *Surf. Sci.*, vol. 149, 1985, pp. 326–340.

34. Kubaschewski, O.; and Alcock, C. B.: *Metallurgical Thermochemistry*, Fifth ed. Volume 24 of *Materials Science & Technology*, G. V. Raynor, ed., Pergamon Press, 1979.

35. Gasser, R. P. H.; and Marsay, C. J.: The Reaction of Oxygen With Rhenium. *Surf. Sci.*, vol. 20, 1970, pp. 107–115.

36. Ollis, D. F.; Lintz, H. G.; Pentenero, A.; and Cassuto, A.: Study of Gas-Solid Chemical Interactions by Noble Gas Molecular Beams. *Surf. Sci.*, vol. 26, 1971, pp. 21–40.

37. Holloway, P. H.; and Outlaw, R. A.: The Effects of Temperature Upon NiO Formation and Oxygen Removal on Ni(110). *Surf. Sci.*, vol. 111, 1981, pp. 300–316.

38. Miedema, A. R.: The Heat of Formation of Alloys. *Philips Tech. Rev.*, vol. 36, no. 8, 1976, pp. 217–231.

39. Holloway, P. H.: Thickness Determination of Ultrathin Films by Auger Electron Spectroscopy. *J. Vac. Sci. & Technol.*, vol. 12, no. 6, Nov./Dec. 1975, pp. 1418–1422.

40. Wagner, C. D.; Riggs, W. M.; Davis, L. E.; Moulder, J. F.; and Muilenberg, G. E., ed.: *Handbook of X-Ray Photoelectron Spectroscopy*. Perkin-Elmer Corp., 1979.

41. Eberhart, M. E.: Modeling Hydrogen Diffusion in Transition Metal Aluminides. Paper presented at 5th NASA-DOE Workshop on Hydrogen-Material Interactions (Scottsdale, AZ), Sept. 23–25, 1992.

Table 1. Normalized Auger Signal as a Function of Depth

[Based on eq. (1)]

Depth, nm	Total Auger signal generated within sample depth (inelastic mean free path of 0.6 nm), percent
0.3	39
.6	63
.9	78
1.2	86
1.5	92
1.8	95
2.1	97
2.4	98

Table 2. Free Energies of Formation of Mo and Re Oxides at 100°C

Compound	Gibb's free energy (est), kcal/g-mol
MoO_2	−144.96
MoO_3	−185.03
Re_2O_7	−316.88
ReO_2	−108.99
ReO_3	−153.20

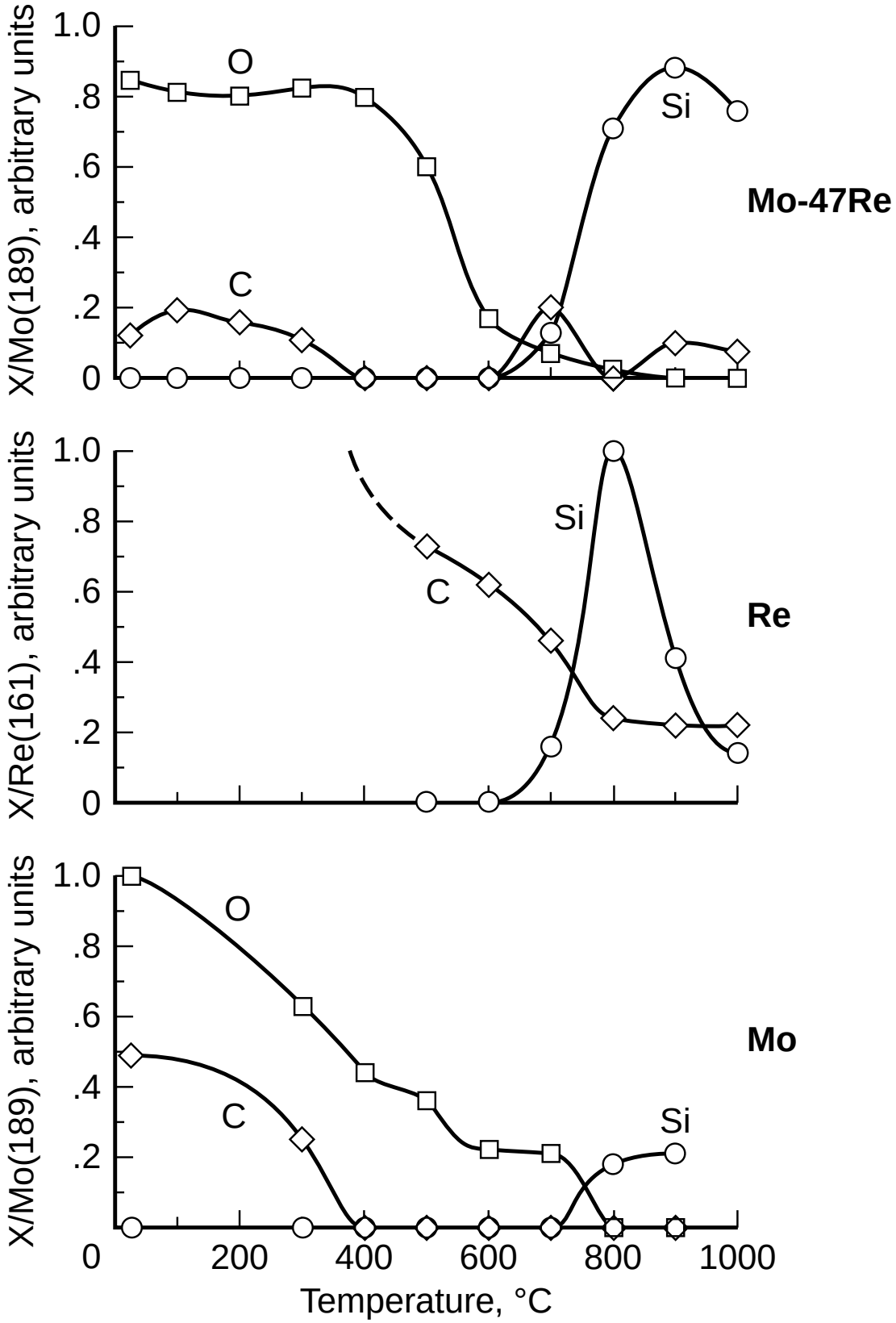

Figure 6. Surface AES compositional changes as function of temperature for as-received samples of Mo-47Re, rhenium, and molybdenum.

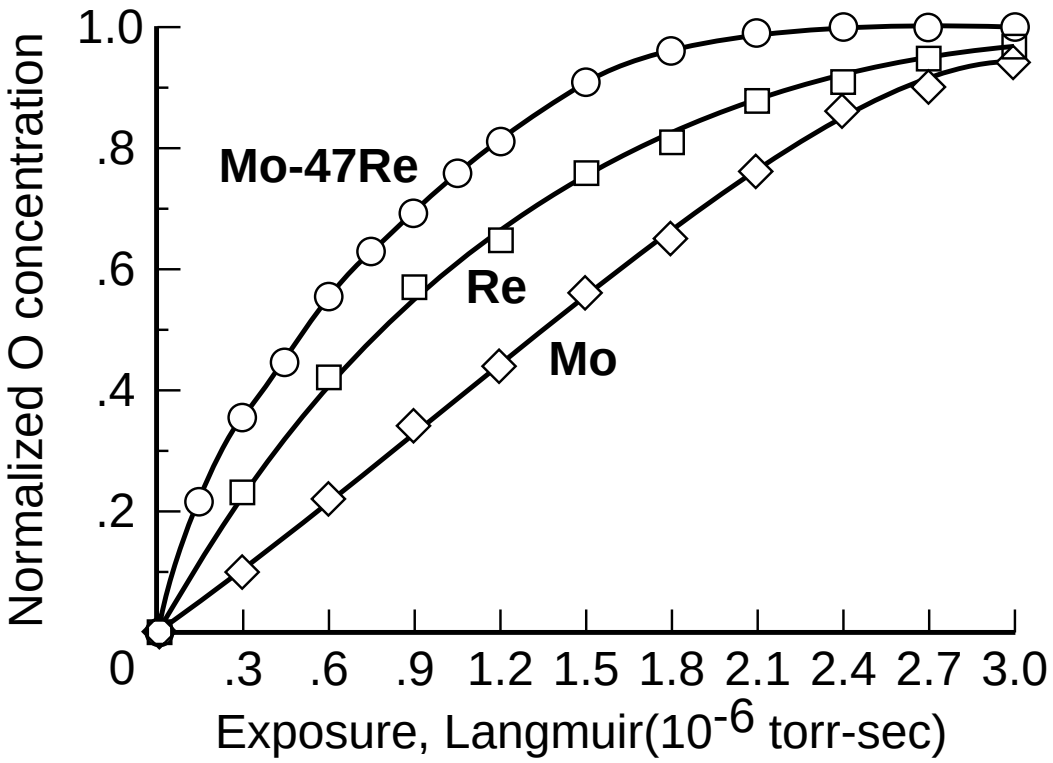

Figure 9. Oxygen (normalized) adsorption curves for Mo-47Re, rhenium, and molybdenum. Adsorption conditions are 3×10^{-9} torr oxygen at 50°C.

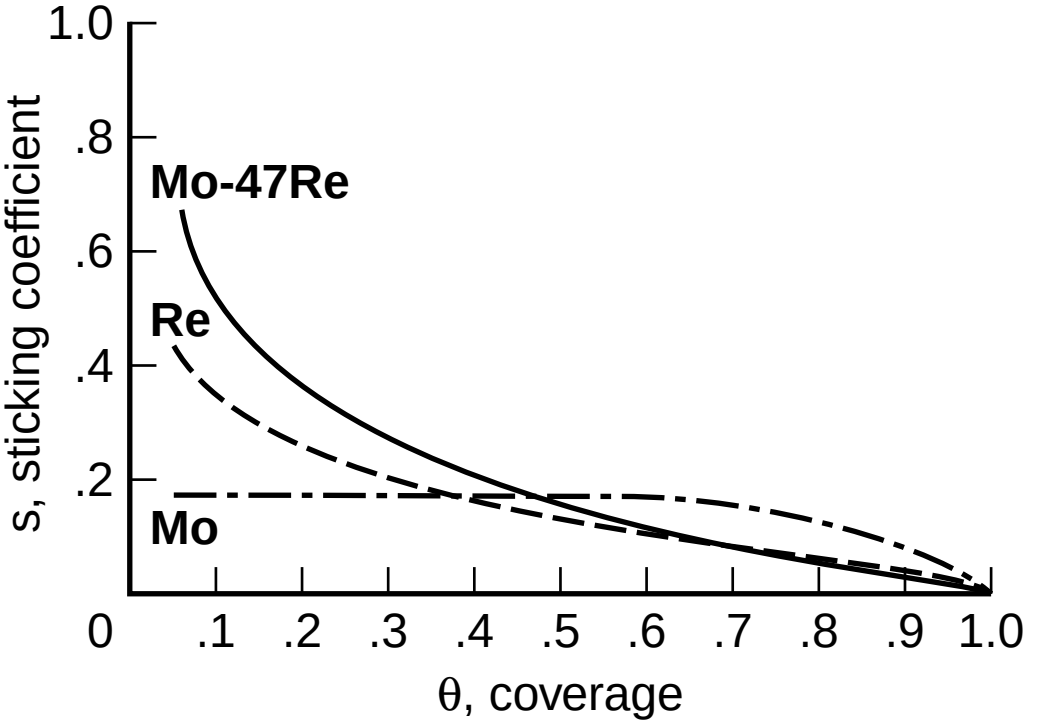

Figure 10. Sticking coefficient as function of coverage for oxygen on Mo-47Re, rhenium, and molybdenum.

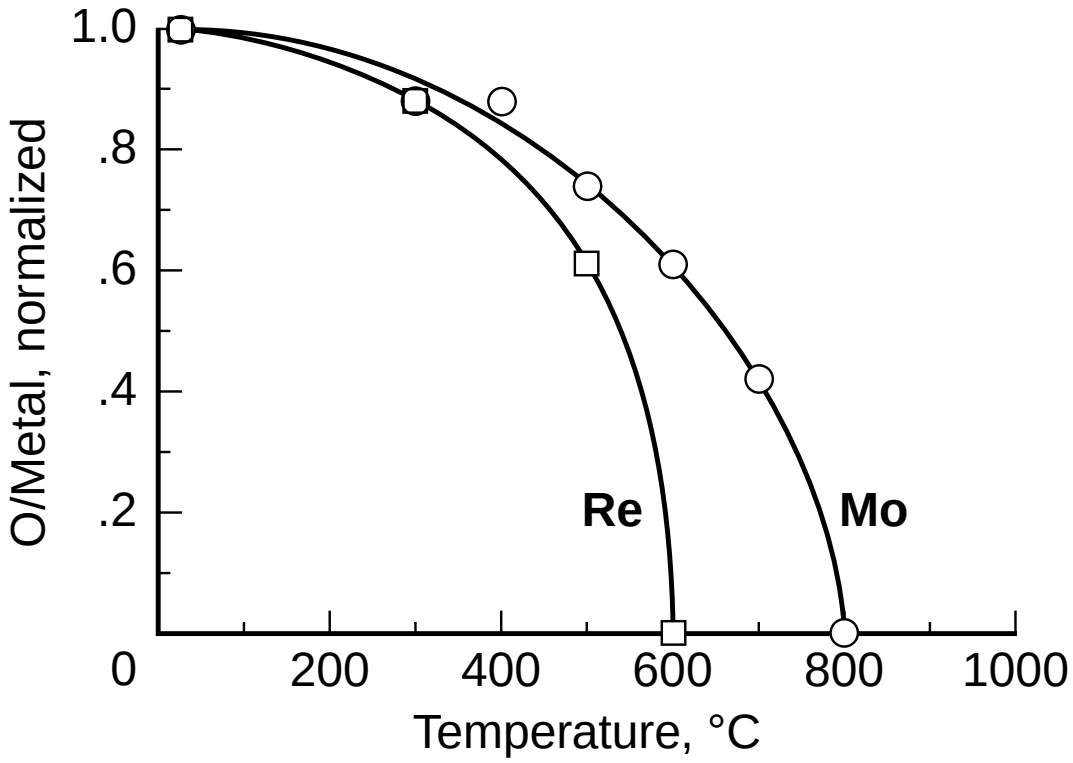

Figure 11. Oxygen (normalized) disappearance curves for rhenium and molybdenum as function of temperature.

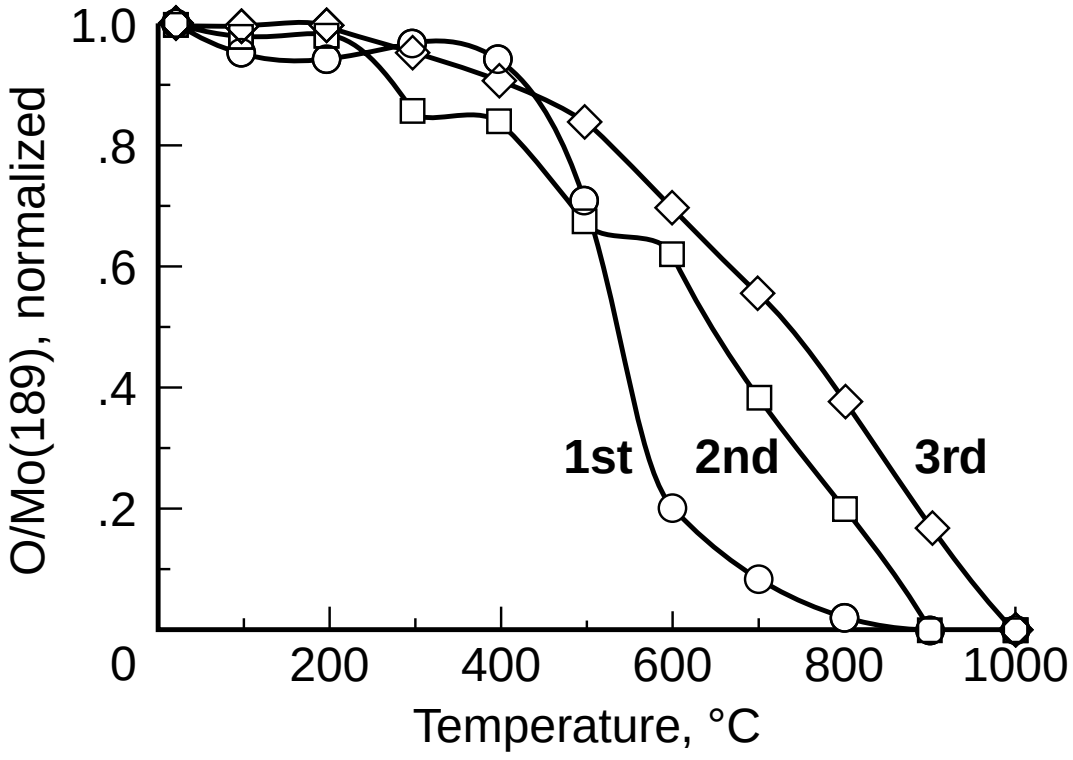

Figure 12. Successive oxygen (normalized) disappearance curves for Mo-47Re as function of temperature.

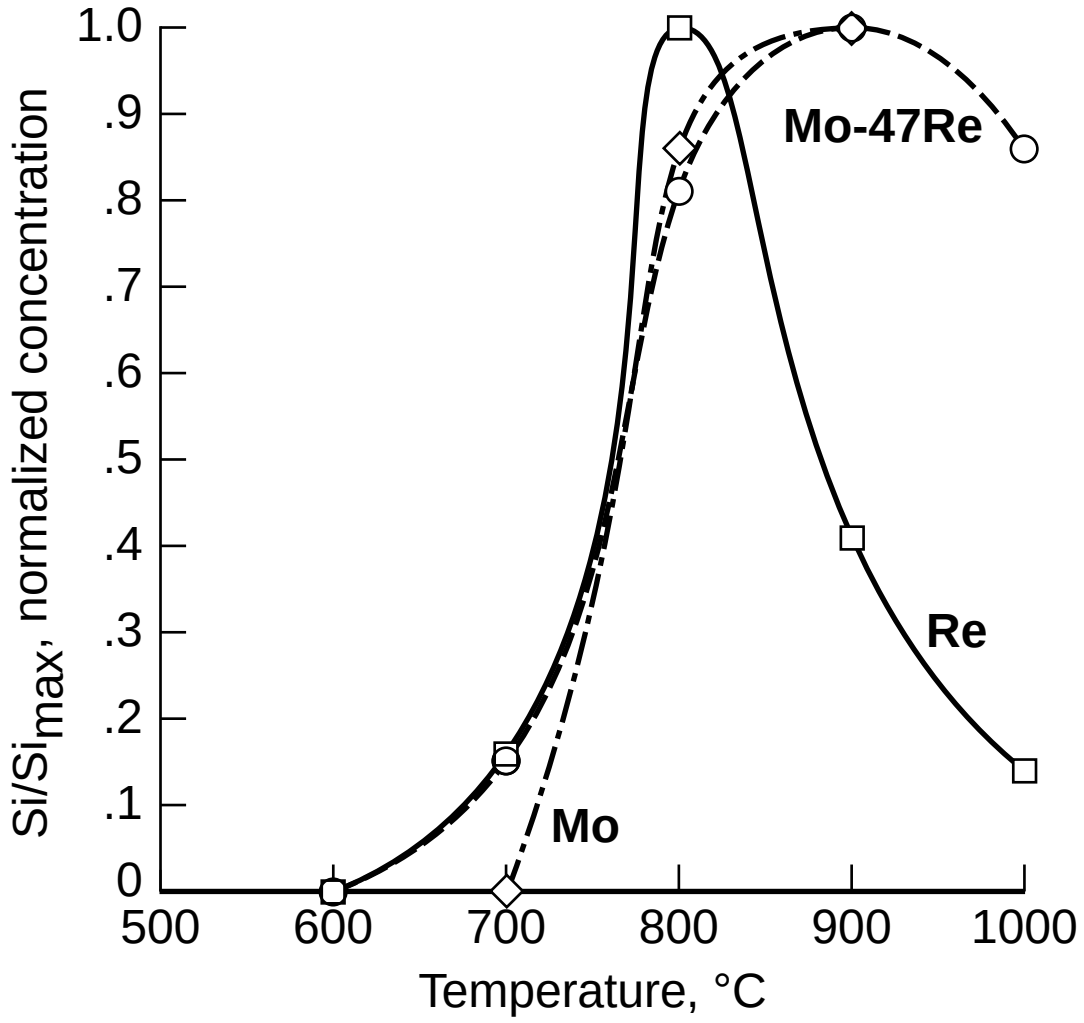

Figure 16. Segregated silicon (normalized) surface concentration (AES) as function of temperature for Mo-47Re, rhenium, and molybdenum.

Figure 1. Photomicrographs of polished and etched Mo-47Re, molybdenum, and rhenium.

Figure 2. AES survey spectrum of polished and etched as-received Mo-47Re alloy.

Figure 3. Forward-scattered and backscattered ISS ($^4He^+$) spectra taken from same as-received sample as that used for figure 2.

Figure 4. High-resolution XPS spectra from same as-received sample as that used for figure 2. Molybdenum ^3D and rhenium ^4F transitions are presented.

(a) AES spectrum.

Figure 5. AES survey spectrum of polished and etched as-received rhenium and backscattered ISS ($^4He^+$) spectra taken from same as-received sample at room temperature and at 300°C.

(b) Backscattered ISS ($^4He^+$) spectra.

Figure 5. Concluded.

Figure 7. AES survey spectra of sputter-cleaned Mo-47Re, rhenium, and molybdenum.

Figure 8. AES survey spectra of oxygen-saturated chemisorption on Mo-47Re, rhenium, and molybdenum.

Figure 13. Low-energy AES (0 to 60 eV) molybdenum peak changes for Mo-47Re surfaces sputter cleaned, O_2 dosed to saturation, and annealed at 1000°C and then cooled to room temperature.

Figure 14. Low-energy AES (0 to 60 eV) Mo peak changes for Mo-47Re surface O_2 dosed to saturation and heated from 300°C to 800°C.

Figure 15. Mid-energy AES (100 to 150 eV) Mo peak changes for molybdenum and Mo-47Re surfaces sputter cleaned, O_2 dosed to saturation, and annealed at 1000°C and then cooled to room temperature.

Figure 17. AES survey spectra of Mo-47Re surfaces O_2 dosed to saturation in presence or absence of silicon segregant.

Figure 18. EELS spectra of O_2 dosed to saturation surface of silicon segregated Mo-47Re as function of temperature.

Figure 19. Backscattered ISS ($^4He^+$) spectra of O_2 dosed to saturation surface of silicon segregated Mo-47Re as function of temperature.

Figure 20. Mid-energy AES (100 to 200 eV) spectrum of molybdenum appearing through platinum-clad Mo-47Re after heating in vacuum to 800°C for 3 hours.

REPORT DOCUMENTATION PAGE

Form Approved
OMB No. 0704-0188

1. AGENCY USE ONLY *(Leave blank)*	2. REPORT DATE	3. REPORT TYPE AND DATES COVERED
	December 1993	Technical Paper

4. TITLE AND SUBTITLE
Surface Compositional Variations of Mo-47Re Alloy as a Function of Temperature

5. FUNDING NUMBERS
WU 763-23-45

6. AUTHOR(S)
S. J. Hoekje, R. A. Outlaw, and S. N. Sankaran

7. PERFORMING ORGANIZATION NAME(S) AND ADDRESS(ES)
NASA Langley Research Center
Hampton, VA 23681-0001

8. PERFORMING ORGANIZATION REPORT NUMBER
L-17278

9. SPONSORING/MONITORING AGENCY NAME(S) AND ADDRESS(ES)
National Aeronautics and Space Administration
Washington, DC 20546-0001

10. SPONSORING/MONITORING AGENCY REPORT NUMBER
NASA TP-3402

11. SUPPLEMENTARY NOTES
Hoekje and Sankaran: Analytical Services & Materials, Hampton, VA; Outlaw: Langley Research Center, Hampton, VA.

12a. DISTRIBUTION/AVAILABILITY STATEMENT
Unclassified–Unlimited

Subject Category 26

12b. DISTRIBUTION CODE

13. ABSTRACT *(Maximum 200 words)*

Molybdenum-rhenium alloys are candidate materials for the National Aero-Space Plane (NASP) as well as for other applications in generic hypersonics. These materials are expected to be subjected to high-temperature (above 1200°C) casual hydrogen (below 50 torr), which could potentially degrade the material strength. Since the uptake of hydrogen may be controlled by the contaminant surface barriers, a study of Mo-47Re was conducted to examine the variations in surface composition as a function of temperature from 25°C to 1000°C. Pure molybdenum and rhenium were also examined and the results compared with those for the alloy. The analytical techniques employed were Auger electron spectroscopy, electron energy loss spectroscopy, ion scattering spectroscopy, and X-ray photoelectron spectroscopy. The native surface was rich in metallic oxides that disappeared at elevated temperatures. As the temperature increased, the carbon and oxygen disappeared by 800°C and the surface was subsequently populated by the segregation of silicon, presumably from the grain boundaries. The alloy readily chemisorbed oxygen, which disappeared with heating. The disappearance temperature progressively increased for successive dosings. When the alloy was exposed to 800 torr of hydrogen at 900°C for 1 hour, no hydrogen interaction was observed.

14. SUBJECT TERMS	15. NUMBER OF PAGES
Sulfur; Segregation; Titanium	30
	16. PRICE CODE: A03

17. SECURITY CLASSIFICATION OF REPORT	18. SECURITY CLASSIFICATION OF THIS PAGE	19. SECURITY CLASSIFICATION OF ABSTRACT	20. LIMITATION OF ABSTRACT
Unclassified	Unclassified		